CNS Neuroscience & Therapeutics

ORIGINAL ARTICLE

CNS Neuroscience & Therapeutics

Morphological Changes of Amygdala in Turner Syndrome Patients

Shu-Yu Li,[1] Yong-Qi Xie,[1] Han Li,[1] Xin-Wei Li,[1] Zhi-Xin Zhang,[2] Qiu-Ling Zhao,[2] Sheng Xie[3] & Gao-Lang Gong[4]

1 School of Biological Science & Medical Engineering, Beihang University, Beijing, China
2 Department of Pediatrics, China-Japan Friendship Hospital, Beijing, China
3 Department of Radiology, China-Japan Friendship Hospital, Beijing, China
4 State Key Laboratory of Cognitive Neuroscience and Learning & IDG/McGovern Institute for Brain Research, Beijing Normal University, Beijing, China

Keywords
Amygdala; MRI; Shape analysis; Turner syndrome.

Correspondence
Gao-Lang Gong, Ph.D., State Key Laboratory of Cognitive Neuroscience and Learning, Beijing Normal University, #19 Xinjiekouwai Street, Beijing 100875, China.
Tel.: +86 10 58804678;
Fax: +86 10 58806154;
E-mail: gaolang.gong@bnu.edu.cn
Received 14 April 2015; revision 2 October 2015; accepted 17 October 2015

doi: 10.1111/cns.12482

SUMMARY

Aims: Turner's syndrome (TS) losts one of the X chromosomes and exhibits social cognition deficits. Previous studies have reported that women with TS demonstrated structural and functional abnormalities in brain, including increased volume in amygdala. However, most studies regarded the amygdala as a whole, and the abnormalities in the specific subregions of amygdala in TS have not been studied. Here, we aimed to investigate the local morphological changes of amygdala in TS using the surface morphology analysis method. **Methods:** A total of 19 adolescents with 45XO TS and 20 matched adolescents with typical development were evaluated using magnetic resonance imaging. The amygdalae of all participants were manually delineated. 3D surface remodeling and parameterization were performed based on the outlined boundaries of amygdalae. We extracted two surface metrics, namely direct Euclidean displacement and normal projection that were used to represent the morphology of amygdala. **Results:** Statistical analysis showed significant outward deformation in the laterobasal subregion of left amygdala in patients with TS, compared with the controls using either direct Euclidean displacement or normal displacement. **Conclusions:** Our findings provide novel insight into the pathological changes in the amygdala of patients with TS.

Introduction

Turner's syndrome (TS) is a common sex chromosome disorder, with the absence of a complete or partial X chromosome in female. Patients with TS have typical physical abnormalities, such as short stature, secondary sexual characteristics dysplasia, and congenital lymphedema [1]. In addition, recent studies have reported the abnormalities in social cognition, involving in facial impressions recognition, emotional stimuli processing and eye gaze perception in women with TS [2–4]. Amygdala plays a major role in emotional processing, for instance fear [5], angry [6,7], and threatening situation [8]. It is also considered to be related with social cognition, particularly emotion recognition and gaze perception [9]. Previous neuroimaging studies have found the enlarged amygdala in patients with TS compared with controls [10–12]. For instance, using volumetric analysis of structural magnetic resonance imaging, researchers found bilateral larger amygdala of women with TS than controls [10,11]. Kesler and colleagues reported the increased volume in left amygdala in patients with TS compared with controls [12].

However, the amygdala is not a homogeneous structure, and it can be divided into three subregions, that is, laterobasal group (LB), centromedial group (CM), and superficial group (SF), according to a histological atlas [13]. Compared with the traditional volumetric analysis method, surface morphology analysis can reveal subtle deformations on the surface of anatomical objects by shape modeling approaches [10]. A number of studies have explored the surface morphology of cerebral structures, such as hippocampus [11,14,15], the central sulcus [16], and amygdala [17–21]. Surface morphology analysis could detect subtle differences on the surface of various brain structures across subjects under neurological disorders. For example, Tamburo and colleagues captured no differences in amygdala volume between the patients with late-life depression and controls, but significant differences in the subfield shape of amygdala by the method of surface analysis [22]. Similarly, Posener and colleagues found highly significant shape differences on the surface of hippocam-

pus, however no significant volume differences between depressed patients and normal subjects [23]. Kim and colleagues suggested the children with autism spectrum disorder had larger laterobasal subregions of amygdala, relative to controls [24]. However, it is largely unknown whether there are surface morphological changes in the amygdala of patients with TS compared with the controls.

Here, we employed a surface-based shape analysis approach to investigate the morphology of amygdala in patients with TS. Using high-resolution structural magnetic resonance (MR) image, the outline of amygdala for each subject was delineated manually, followed by parameterization and three-dimensional spherical harmonic description. Two-sample *t*-test was applied to detect the significant between-group differences in the surface of amygdalae.

Materials and Methods

Participants

The subjects included 19 adolescents with 45XO TS and 20 adolescents with typical development, matched for ages (as showed in Table 1). All patients with TS were monosomic females with a 45XO karyotype, who were recruited from the China-Japan Friendship Hospital (CJFH) and Peking Union Medical College Hospital (PUMCH). Control subjects were recruited through local community and parent networks. For each participant, the cognitive assessments were performed within 2 days prior to or after the MRI scan. The participants were assessed with the Chinese version of the Wechsler Intelligence Scale for Children-Fourth Edition (WISC-IV) [25]. The demographic data of all participants are demonstrated in Table 1. All participants had no history of neurological and psychiatric diseases. The research protocol was approved by the Research Ethics Committee of the Beijing Normal University. For each participant, informed written consent was obtained from the legal guardian.

Image Acquisition and Preprocessing

All subjects were scanned on the same 3.0 T Siemens Tim Trio MRI scanner in the Imaging Center for Brain Research, Beijing Normal University. High-resolution 3D T1-weighted images were acquired through magnetization prepared rapid gradient echo (MPRAGE) sequence with the following parameters: echo time (TE) = 3.39 ms; repletion time (TR) = 2530 ms; inversion time (TI) = 1100 ms; matrix = 256 × 256; in-plane resolution = 1 × 1 mm; 176 sagittal slices; thickness = 1 mm; and FA = 7°.

All original MR images were registered into stereotaxic space by a linear transformation firstly [26,27]. At the same time, we used the N3 algorithms to correct nonuniformity artifacts for all images [28].

Table 1 Subject demographics

	Turner's syndrome (n = 19)	Normal control (n = 20)	*P*
Age (years), mean ± SD	14.0 ± 2.8 (10.2–18.6)	13.9 ± 2.2 (9.9–17.5)	0.447
IQ, mean ± SD	110.2 ± 14.9	88.9 ± 16.9	<0.001

Manual Delineation of Amygdala

Two raters were blind to diagnosis when tracing the amygdala boundary in coronal slices using itk-SNAP (http://www.itk-snap.org) software. This software allows raters to examine the three orthogonal planes together. The amygdala was extracted according to the anatomical definition of amygdala that was described by the Center for Interdisciplinary Brain Sciences Research (CIBSR) at the Stanford University School of Medicine (http://cibsr.stanford.edu) [29]. We used the same criteria with the previous literature, which has the detailed descriptions on the definition of amygdala boundary. Briefly, the most anterior slice of the amygdala was located where anterior commissure (AC) was clearest (thickest, longest, and most continuous). The inferior boundary was formed by a white matter tract at the bottom of the amygdala (as show in Figure 1A). The medial border was always marked by white matter or cerebrospinal fluid (CSF). The superior border of the amygdala was delineated by either high-intensity white matter or CSF (as showed in Figure 1B). Moreover, the lateral border of the amygdala was defined by dense, central white matter tract of the temporal lobe. It was challenging that the amygdala and hippocampus both appeared in the transition (jumping) slice. On these slices, the temporal horn started to enlarge more superiorly along the lateral side of the two structures, and we could divide the two structures by a white matter trace or CSF (as showed in Figure 1C). Raters must examine these slices carefully and discern the amygdala and hippocampus accurately, in the meanwhile, referring to the sagittal view [13] (as showed in Figure 1D).

It is necessary to check the reliability of the manual outlining in order to eliminate the influence of raters' subjectivity. Two raters who were blind to the side of the brain (left or right) traced the boundary of amygdala on five randomly selected brain volumes. Correlation coefficients between the raters were, respectively, 0.91 and 0.90 for the volumes of left and right amygdala. Six months later, one rater repeated to trace the boundary of amygdala on five randomly selected brains, and the intrarater correlation coefficients for the left and right amygdala were 0.97 and 0.96, respectively.

Surface Modeling and Registration

We utilized the software of SPHARM Modeling and Analysis Toolkit (SPHARM-MAT) (http://www.iupui.edu/&shenlab) which created parametric surface models using spherical harmonics to perform the surface reconstruction of the amygdala [30]. The spherical harmonics description method was a powerful shape descriptor to pinpoint regional changes in morphology. Our surface morphology analysis was based on this method.

As SPHARM-MAT can only be used to model arbitrarily shaped but simply connected 3D objects, each of the manually segmented 3D binary images needed to have a spherical topology before surface reconstruction. Then, the fixed images were parameterized based on spherical mapping, where a con-

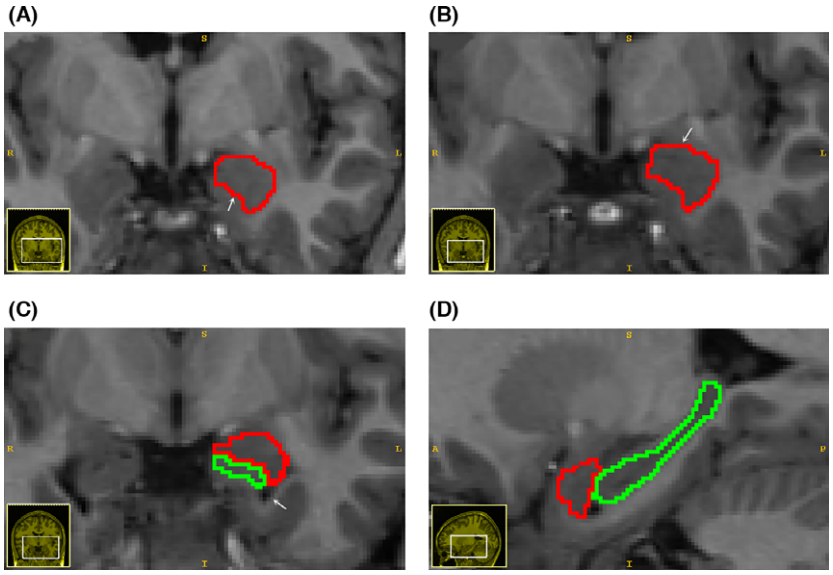

Figure 1 Manual delineation of the amygdala. (**A**) The left amygdala section in the coronal plane. The red line indicates the border of amygdala and white arrow marks its inferior boundary on coronal plane. In the bottom left corner of the figure is the thumbnail on coronal plane. L and R indicate the left and right side, respectively. (**B**) The left amygdala section in the coronal plane. The red line indicates the border of amygdala and white arrow marks its superior boundary on coronal plane. (**C**) The left amygdala and hippocampus section in the coronal plane. The red line indicates the border of amygdala and green line represents outline of hippocampus, the white arrow marks the temporal horn which starts to enlarge distinctly along the lateral side of the two structures. (**D**) The left amygdala and hippocampus sections in the sagittal plane. The red line indicates the border of amygdala and green line represents the outline of hippocampus. In the bottom left corner of the figure is the thumbnail on sagittal plane. A and P indicate the anterior and posterior side, respectively.

tinuous and uniform mapping from the object surface to the surface of a unit sphere was created with spherical parameterization. Simultaneously, we used the method of Control of Area and Length Distortions (CALD), which minimized the area distortion cost (ADC) and controlled its worst length distortion cost (LDC) at the same time. Each vertex on the surface was represented by a pair of coordinates after the parameterization. Then, the object surface was expanded into a complete set of spherical harmonic basis functions that were essentially Fourier basis functions defined on the sphere. The Fourier coefficients of the spherical harmonic basis functions that were up to a user-desired degree could be used to reconstruct the object surface while using more coefficients led to a more detailed reconstruction [31].

Surface alignment was an important procedure allowing for pairwise processing or group analysis across different surface models and could facilitate the comparison between the parameter space and object space. This procedure in our experiment mainly included three steps. Firstly, we conducted the first order ellipsoid (FOE) alignment that was performed by selecting the first order spherical harmonic coefficients. Given that the final results of FOE alignments did not preserve the original geometric information in the object space, further alignment was needed. Then, all the intermediate results of the FOE alignment in each side of the amygdala were averaged to generate the corresponding template atlas. Finally, SPHARM Registration with ICP (SHREC) algorithm was used to perform further alignment of the surface of right or left amygdala by minimizing the mean square distances between the corresponding points in the individual surface and template [31].

Surface Metrics

We employed two widely used surface metrics to localize shape changes between individual amygdala and the template. One of the surface metrics was the Euclidean distance from each surface vertex in the subjects to the evenly distributed template [21].The other surface metric was defined as the distance between each vertex of the subject and the corresponding vertex in the template surface along the normal direction of the mean surface [32]. The positive value of the metrics indicated an outward deformation in the subregion of the subject, relative to the corresponding region of average surface and vice versa. Finally, we used a 5 mm surface-based diffusion smoothing kernel to blur the metric map [33].

Statistical Analysis

For each surface metric, we used a multiple linear regression model to explore the between-group differences vertex by vertex, with age and IQ as covariates. We also evaluated the interaction effects between the group and age. We applied random field theory for multiple comparison corrections on the entire surface [34]. P values <0.05 (FWE-corrected, cluster level) were considered to

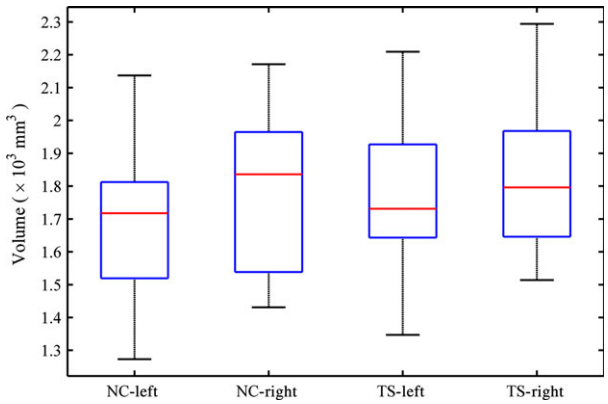

Figure 2 The box plot of bilateral amygdala volumes in normal control (NC) and Turner's syndrome (TS) groups.

be statistically significant. Here, SurfStat (http://www.-math.mcgill.ca/keith/surfstat/) was applied to implement the statistical analysis.

Results

Amygdala Volumetry

We computed the number of voxels in the mask of manually segmented amygdala as the volume for left and right amygdala. The volume of the subjects with TS was 1761 ± 214 mm^3 for left amygdala and 1810 ± 205 mm^3 for right amygdala. And the volume of control group was 1694 ± 217 mm^3 and 1780 ± 227 mm^3 for left and right amygdala, respectively. The box plot of amygdala volumes is shown in Figure 2. There were no significant volume differences between the left and right amygdala between the two groups (all $P > 0.05$).

Local Shape Variation

We computed the between-group differences in direct displacement on the surface of amygdala in vertex-by-vertex style. The regions showing significant differences were located in the LB part of the left amygdala. Specifically, the participants with TS showed larger outward deformation, compared with normal controls. The results are illustrated in Figure 3. Figure 3A,B is the scenographs of left amygdala on the coronal plane. The amygdala was displayed from the direction of anterior to posterior. The significant surface cluster ($P < 0.01$, cluster level, corrected) was colored. Figure 3C, D is the back views of Figure 3A,B. Notably, right amygdala did not show any significant differences between the two groups. Using normal displacement, we observed the similar results (see Figure 4). Notably, for each of the surface metrics, we did not find any significant interaction effect between the group and age.

Discussion

In this study, we employed a surface shape analysis method to investigate the abnormal changes of subregional morphology of amygdala in patients with TS. There were no significant differences in bilateral amygdala volumes between the TS and control group. However, we found outward deformations in the LB of the left amygdala surface in the TS group compared with the normal controls. These results provide new insight into the neuropathological basis of TS.

There were some studies reporting the amygdala volume changes in TS groups, and the findings were still inconsistent. For instance, Kesler and colleagues found an increased volume of the left amygdala in 45XO TS compared with the controls [12]. Other studies suggested significant enlargements of bilateral amygdalae for the participants with 45XO TS [10,11]. In contrast, Cutter and colleagues found no significant differences in volumes of the left and right amygdala between the patients with TS and the controls

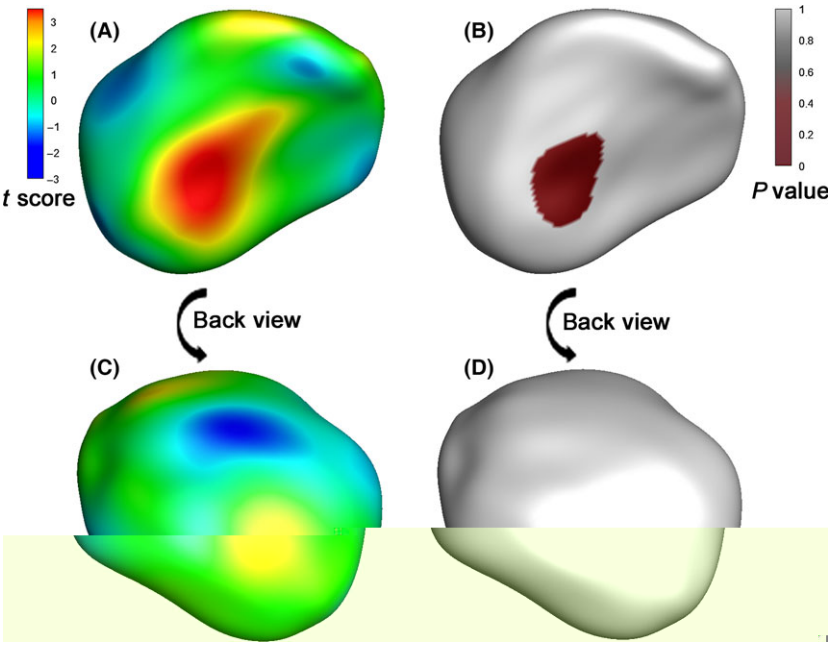

Figure 3 The results of surface morphology analysis using direct displacement as the surface metric. (**A**) The scenograph of left amygdala on the coronal plane. The figure is shown from direction of anterior to posterior. Ventral view of *t*-test scores between Turner's syndrome (TS) group and controls. (**B**) The scenograph of left amygdala on the coronal plane. The figure is shown from direction of anterior to posterior. Ventral view of *P* value between TS group and controls. Only significant surface clusters ($P < 0.01$, cluster level, corrected) are colored. (**C**) Dorsal view of *t*-test scores between TS group and controls. (**D**) Dorsal view of *P* value between TS group and controls. Notably, right amygdala was not shown as no significant result was found.

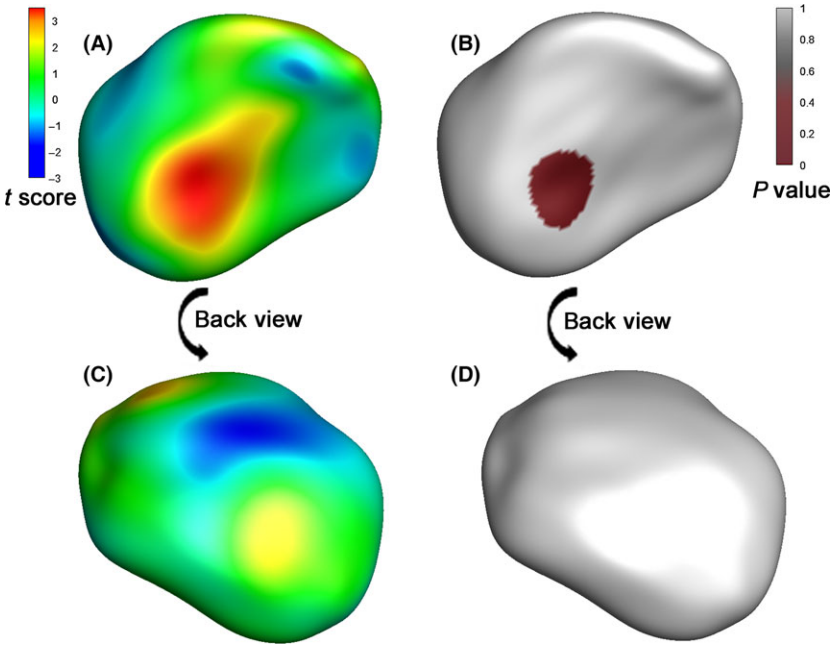

Figure 4 The results of surface morphology analysis using normal displacement as the surface metric. (**A**) The scenograph of left amygdala on the coronal plane. The figure is shown from direction of anterior to posterior. Ventral view of *t*-test scores between Turner's syndrome (TS) group and controls. (**B**) The scenograph of left amygdala on the coronal plane. The figure is shown from direction of anterior to posterior. Ventral view of *P* value between TS group and controls. Only significant surface clusters ($P < 0.01$, cluster level, corrected) are colored. (**C**) Dorsal view of *t*-test scores between TS group and controls. (**D**) Dorsal view of *P* value between TS group and controls. Notably, right amygdala was not shown as no significant result was found.

[35]. Our findings were in line with the results of Cutter and colleauges. However, we found the outward deformations of the left amygdala surface in TS. One possible reason for this finding is that the local deformation changes in patients with TS may be too subtle to make the change of entire volume notable.

In our study, the observed significant changes in the TS group were mainly located around the LB of the left amygdala, which mainly consists of the lateral and basolateral nucleus. The LB is associated with reception of visual information stimulus including facial expression and gaze direction, and fear response. Converging evidence indicated that the LB could integrate visual information, and had axonal connections with visual areas in monkey studies [36–38]. Recently, *in vivo* study in human demonstrated that the LB of human amygdala is the hub for visual information input processing [39]. The LB is believed to receive related inputs from the cortical and subcortical regions, and sends outputs to other subregions of amygdala and other brain structures [40]. Skuse and colleagues suggested that the left and right amygdala played distinct, but complementary, roles in fearful emotion recognition [41], and the left amygdala activation was more likely associated with the discrimination of facial expression and cognitive processing [41–43]. Hurlemann and colleagues further demonstrated that the LB of the left amygdala was associated with facial emotion perception in a functional MRI study [42]. Recently, some studies have found aberrant social cognition in women with TS, involving fearful face recognition and eye gaze processing [4,41,43]. Particularly, the changed behaviors were related to the amygdala development. Our findings on outward deformation of the LB in the left amygdala therefore provide further support to the notion that the LB of the left amygdala plays a significant role in fearful emotion recognition and gaze perception.

Some issues need to be considered. First, the cerebral pathological changes in TS would be affected by genomic imprinting. Individuals with TS who preserved the maternal X chromosome (45, Xm) and individuals with TS who preserved the paternal X chromosome (45, Xp) had distinct anatomical structure and psychosocial functioning [44,45]. Thus,it is better to take genomic imprinting into consideration in the future. Second, in this study, we did not include any clinical measures for our subjects. It therefore limited our ability to determine the clinical relevance of our findings on structural alterations of amygdala. Third, our study contained a small sample size of subjects, resulting in a limited statistical power. Fourth, we used manual segmentation to outline the boundaries of amygdalae, but it is time-consuming and heavy workload. In future, it would be interesting to compare the results using manual segmentation and automatic segmentation methods, such as FSL/FIRST or Freesurfer software (http://surfer.nmr.mgh.harvard.edu/).

Conclusion

In this study, we found surface outward deformation of the LB in the left amygdala in adolescents with TS, compared with healthy controls. This particular abnormalities may underlie impaired social cognition in TS, including fearful facial impressions recognition and eye gaze perception. This findings may be useful to enhance our understanding about the pathological changes of the amygdala in patients with TS.

Acknowledgment

This work was supported by the 973 program (2013CB837300), the National Science Foundation of China (Nos. 81271649, 81471731, and 81322021), the Beijing Nova Program (Z121110002512032), and the Fundamental Research Funds for the Central Universities.

Conflict of Interest

The authors declare no conflict of interest.

References

1. Agrawal N, Gupta M, Wangnoo S. Turner's syndrome. *Apollo Med* 2009;**6**:335–339.
2. Skuse DH. X-linked genes and mental functioning. *Hum Mol Genet* 2005;**14**:R27–R32.
3. Molko N, Cachia A, Riviere D, et al. Brain anatomy in Turner syndrome: Evidence for impaired social and spatial–numerical networks. *Cereb Cortex* 2004;**14**:840–850.
4. Lawrence K, Kuntsi J, Coleman M, Campbell R, Skuse D. Face and emotion recognition deficits in Turner syndrome: A possible role for X-linked genes in amygdala development. *Neuropsychology* 2003;**17**:39.
5. Phelps EA, O'Connor KJ, Gatenby JC, Gore JC, Grillon C, Davis M. Activation of the left amygdala to a cognitive representation of fear. *Nat Neurosci* 2001;**4**:437–441.
6. Stein MB, Goldin PR, Sareen J, Zorrilla LTE, Brown GG. Increased amygdala activation to angry and contemptuous faces in generalized social phobia. *Arch Gen Psychiatry* 2002;**59**:1027–1034.
7. Monk CS, Telzer EH, Mogg K, et al. Amygdala and ventrolateral prefrontal cortex activation to masked angry faces in children and adolescents with generalized anxiety disorder. *Arch Gen Psychiatry* 2008;**65**:568–576.
8. Hyde LW, Gorka A, Manuck SB, Hariri AR. Perceived social support moderates the link between threat-related amygdala reactivity and trait anxiety. *Neuropsychologia* 2011;**49**:651–656.
9. Mcgaugh JL. The amygdala modulates the consolidation of memories of emotionally arousing experiences. *Annu Rev Neurosci* 2004;**27**:1–28.
10. Good CD, Lawrence K, Thomas NS, et al. Dosage-sensitive X-linked locus influences the development of amygdala and orbitofrontal cortex, and fear recognition in humans. *Brain* 2003;**126**:2431–2446.
11. Lepage J-F, Mazaika PK, Hong DS, Raman M, Reiss AL. Cortical brain morphology in young, estrogen-naive, and adolescent, estrogen-treated girls with Turner syndrome. *Cereb Cortex* 2013;**23**:2159–2168.
12. Kesler SR, Garrett A, Bender B, Yankowitz J, Zeng SM, Reiss AL. Amygdala and hippocampal volumes in Turner syndrome: A high-resolution MRI study of X-monosomy. *Neuropsychologia* 2004;**42**:1971–1978.
13. Amunts K, Kedo O, Kindler M, et al. Cytoarchitectonic mapping of the human amygdala, hippocampal region and entorhinal cortex: Intersubject variability and probability maps. *Anat Embryol* 2005;**210**:343–352.
14. Cates J, Fletcher PT, Styner M, Hazlett HC, Whitaker R. Particle-based shape analysis of multi-object complexes. *Med Image Comput Comput Assist Interv* 2008;**11**:477–485.
15. Dager S, Wang L, Friedman S, et al. Shape mapping of the hippocampus in young children with autism spectrum disorder. *AJNR Am J Neuroradiol* 2007;**28**:672–677.
16. Golland P, Grimson WEL, Shenton ME, Kikinis R. Detection and analysis of statistical differences in anatomical shape. *Med Image Anal* 2005;**9**:69–86.
17. Yushkevich PA, Avants BB, Pluta J, et al. A high-resolution computational atlas of the human hippocampus from postmortem magnetic resonance imaging at 9.4 T. *NeuroImage* 2009;**44**:385–398.
18. Li S, Han Y, Wang D, et al. Mapping surface variability of the central sulcus in musicians. *Cereb Cortex* 2010;**20**:25–33.
19. Chung MK, Worsley KJ, Nacewicz BM, Dalton KM, Davidson RJ. General multivariate linear modeling of surface shapes using SurfStat. *NeuroImage* 2010;**53**:491–505.
20. Qiu A, Miller MI. Multi-structure network shape analysis via normal surface momentum maps. *NeuroImage* 2008;**42**:1430–1438.
21. Kim N, Kim HJ, Hwang J, et al. Amygdalar shape analysis method using surface contour aligning, spherical mapping, and probabilistic subregional segmentation. *Neurosci Lett* 2011;**488**:65–69.
22. Kim HJ, Kim N, Kim S, et al. Sex differences in amygdala subregions: Evidence from subregional shape analysis. *NeuroImage* 2012;**60**:2054–2061.
23. Peterson BS, Choi HA, Hao X, et al. Morphologic features of the amygdala and hippocampus in children and adults with Tourette syndrome. *Arch Gen Psychiatry* 2007;**64**:1281–1291.
24. Kim JE, Lyoo IK, Estes AM, et al. Laterobasal amygdalar enlargement in 6-to 7-year-old children with autism spectrum disorder. *Arch Gen Psychiatry* 2010;**67**:1187.
25. Wechsler D. *Wechsler Intelligence Scale for Children-Fourth Edition (WISC-IV)*. San Antonio, TX: The Psychological Corporation, 2003.
26. Rey M, Dellatolas G, Bancaud J, Talairach J. Hemispheric lateralization of motor and speech functions after early brain lesion: Study of 73 epileptic patients with intracarotid amytal test. *Neuropsychologia* 1988;**26**:167–172.
27. Collins DL, Neelin P, Peters TM, Evans AC. Automatic 3D intersubject registration of MR volumetric data in standardized Talairach space. *J Comput Assist Tomogr* 1994;**18**:192–205.
28. Sled JG, Zijdenbos AP, Evans AC. A nonparametric method for automatic correction of intensity nonuniformity in MRI data. *IEEE Trans Med Imaging* 1998;**17**:87–97.
29. Karchemskiy A, Garrett A, Howe M, et al. Amygdalar, hippocampal, and thalamic volumes in youth at high risk for development of bipolar disorder. *Psychiatry Res* 2011;**194**:319–325.
30. Brechbühler CM. Description and analysis of 3-D shapes by parametrization of closed surfaces. Diss. Techn. Wiss. ETH Zürich, Nr. 10979, 1995. Ref.: Guido Gerig; Korref.: Nicholas Ayache, 1995.
31. Shen L, Makedon F. Spherical mapping for processing of 3D closed surfaces. *Image Vis Comput* 2006;**24**:743–761.
32. Shen L, Saykin A, McHugh T, et al. Morphometric MRI study of hippocampal shape in MCI using spherical harmonics. *Alzheimers Dement* 2005;**1**:S47.
33. Chung MK, Worsley KJ, Robbins S, et al. Deformation-based surface morphometry applied to gray matter deformation. *NeuroImage* 2003;**18**:198–213.
34. Taylor JE, Adler RJ. Euler characteristics for Gaussian fields on manifolds. *Ann Probab* 2003;**31**:533–563.
35. Cutter WJ, Daly EM, Robertson DM, et al. Influence of X chromosome and hormones on human brain development: A magnetic resonance imaging and proton magnetic resonance spectroscopy study of Turner syndrome. *Biol Psychiatry* 2006;**59**:273–283.
36. Sah P, Faber EL, De Armentia ML, Power J. The amygdaloid complex: Anatomy and physiology. *Physiol Rev* 2003;**83**:803–834.
37. Phelps EA. Emotion and cognition: Insights from studies of the human amygdala. *Annu Rev Psychol* 2006;**57**:27–53.
38. Iwai E, Yukie M. Amygdalofugal and amygdalopetal connections with modality-specific visual cortical areas in macaques (*Macaca fuscata*, *M. mulatta*, and *M. fascicularis*). *J Comp Neurol* 1987;**261**:362–387.
39. Bzdok D, Laird AR, Zilles K, Fox PT, Eickhoff SB. An investigation of the structural, connectional, and functional subspecialization in the human amygdala. *Hum Brain Mapp* 2013;**34**:3247–3266.
40. Phelps EA, LeDoux JE. Contributions of the amygdala to emotion processing: From animal models to human behavior. *Neuron* 2005;**48**:175–187.
41. Skuse D, Morris J, Dolan R. Functional dissociation of amygdala-modulated arousal and cognitive appraisal, in Turner syndrome. *Brain* 2005;**128**:2084–2096.
42. Hurlemann R, Rehme AK, Diessel M, et al. Segregating intra-amygdalar responses to dynamic facial emotion with cytoarchitectonic maximum probability maps. *J Neurosci Methods* 2008;**172**:13–20.
43. Hong DS, Bray S, Haas BW, Hoeft F, Reiss AL. Aberrant neurocognitive processing of fear in young girls with Turner syndrome. *Soc Cogn Affect Neurosci* 2014;**9**:255–264.
44. Mullaney R, Murphy D. Turner syndrome: Neuroimaging findings: Structural and functional. *Dev Disabil Res Rev* 2009;**15**:279–283.
45. Nicholls RD, Knepper JL. Genome organization, function, and imprinting in Prader-Willi and Angelman syndromes. *Annu Rev Genomics Hum Genet* 2001;**2**:153–175.